Morphology and Fracture Behavior of Intercalated Epoxy/Clay Nanocomposites

Tianxi Liu,[1,*] Wuiwui Chauhari Tjiu,[1] Yuejin Tong,[1] Chaobin He,[1] Sok Sing Goh,[2] Tai-Shung Chung[2]

[1]*Molecular and Performance Materials Cluster, Institute of Materials Research and Engineering, 3 Research Link, 117602 Singapore*
[2]*Department of Chemical and Environmental Engineering, The National University of Singapore, 10 Kent Ridge Crescent, 119260 Singapore*

Received 12 November 2003; accepted 26 May 2004
DOI 10.1002/app.21033
Published online in Wiley InterScience (www.interscience.wiley.com).

ABSTRACT: Epoxy/clay nanocomposites were prepared by swelling organoclay in an epoxy resin, diglycidyl ether of bisphenol A, followed by curing with an aromatic hardener, diethyltoluenediamine. A combination of X-ray diffraction with transmission electron microscopy showed the coexistence of intercalated and exfoliated clay morphologies throughout the matrix. In addition, a microscopic and homogeneous dispersion of clay agglomerations, with sizes ranging from about 2 to 5 μm, was revealed by optical microscopy. Dynamic mechanical analysis indicated a steady increase in storage modulus and a gradual decrease in high glass-transition temperature as the clay loading increased. The fracture toughness of the nanocomposites significantly increased with increasing clay concentration, suggesting a toughening effect from the clay particles. Scanning electron microscopy and optical microscopy observations of the epoxy/clay nanocomposites suggested that shear yielding of the matrix, crack deflection, voiding, and debonding of clay particles and epoxy matrix are among the operative toughening mechanisms observed. © 2004 Wiley Periodicals, Inc. J Appl Polym Sci 94: 1236–1244, 2004

Key words: epoxy; clay; nanocomposites; morphology; fracture

INTRODUCTION

Polymer/clay nanocomposite is a new class of materials formed by dispersing clay particles throughout a polymer matrix.[1–3] The fine and homogeneous dispersion of clay endows the nanocomposite with unique properties not shared by other conventional materials, which offers new technological and economic opportunities.[3] This concept was first introduced by the researchers from Toyota, who discovered the possibility of building a nanocomposite from nylon 6 and organophilic montmorillonite clay by *in situ* polymerization.[4,5] The materials developed by Toyota demonstrate dramatic improvements in mechanical and physical properties, which are currently used to make the timing-belt cover of Toyota's car engines and for the production of packaging film. Since then, the high promise for industrial applications has motivated extensive research to disperse clay-type fillers in many other polymeric matrices, such as epoxy,[6–11] polystyrene,[12,13] and so on.

Correspondence to: T. Liu (liu-tx@imre.a-star.edu.sg).
**Present address:* Institute of Advanced Materials, Fudan University, 220 Handan Road, Shanghai 200433, P.R. China.

Journal of Applied Polymer Science, Vol. 94, 1236–1244 (2004)

Epoxies are thermoset polymers having versatility in their chemical forms. Most of the epoxies are widely used as protective coatings and adhesives, whereas others are used in structural applications such as laminates and composites, tooling, molding, casting, electronics, and construction.[14] The characteristics of epoxy resins constitute an excellent combination of chemical and corrosion resistance, and good mechanical and electrical properties. These characteristics, along with a long service life, make epoxies a necessity in the future growth of new technologies. Presently, there is high potential for more sophisticated application of high-performance epoxies in both automotive and aerospace industries. However, epoxies have brittle characteristics that may hinder their potential applications in aerospace and automotive applications. For structural applications, for example, epoxy resins tend to be either brittle or notch sensitive. Therefore, tremendous efforts have been focused on improving the toughness of epoxy systems, which has stimulated an overwhelming interest in filling epoxy with inorganic fillers (such as particulates, fibers, and layered fillers) in the pursuit of toughening epoxy resin.[15–18]

Despite numerous studies on the synthesis and characterization of polymer/clay nanocomposites,[1–3] scant attention has been paid to their fracture behavior and toughening mechanisms.[19–21] In this study, intercalated epoxy/clay nanocomposites were prepared by

in situ polymerization. The aim is to characterize the effect of clay addition on the morphology and mechanical properties (e.g., fracture behavior) of the epoxy nanocomposites. Microscopic approaches were used to investigate the fracture behavior and toughening mechanisms of the materials.

EXPERIMENTAL

Materials

The epoxy resin used was diglycidyl ether of bisphenol-A (DGEBA; DER354 from Dow Chemical Co., Midland, MI), which is a liquid-reaction product of bisphenol-F and epichlorohydrin, with an average epoxide equivalent weight of 175 g. The aromatic hardener, Ethacure 100-A1 (chemical name: diethyltoluenediamine) used here, is a mixture of two diethyltoluene diamine (DETDA) isomers: 50–81% 2,4-isomer and 18–20% 2,6-isomer (from Albermarle Corp., Richmond, VA). The clay used in this study, Cloisite® 93A, is commercially available from Southern Clay Products Inc. (Gonzales, TX), which is basically an organically modified montmorillonite [with cation exchange capacity (CEC) = 90 meq/100 g] with a ternary ammonium salt by an ion-exchange method.

Preparation of epoxy/clay nanocomposites

The clay was dried at 60°C for 24 h under vacuum before sample preparation. The nanocomposite samples, with different clay loadings, were made by mixing the desired amount of clay with the epoxy resin, using a homogenizer at 10,000 rpm for 60 min. This was followed by sonication for about 60 min, using an ultrasonic cleaner, and degassing in the vacuum oven at 70°C. A curing agent was added to the clay/epoxy mixture by stoichiometric ratio. The mixture was then blended under vacuum for another 30 min at 70°C. The mixture of clay, resin, and curing agent was poured into a preheated glass mold that was surface treated with a mold-releasing agent. All samples were vertically mounted in an oven and cured at 75°C for 2.5 h, at 100°C for 2 h, and at 150°C for 1.5 h, followed by a postcuring at 180°C for 3 h. The resulting plates of neat epoxy and nanocomposite samples were 6 mm thick.

Specimen preparation and bending tests

The fracture toughness (i.e., critical stress intensity factor), K_{IC} was measured by fracturing single-edge-notch (SEN) specimens using three-point bending (3PB) tests.[22] The sample plates were machined into specimens with a geometry of $6 \times 12 \times 70$ mm^3. A notch depth equivalent to half the width was created in the center of each rectangular bar using a saw. Before testing, the specimens were precracked by inserting a fresh razor blade into the sawed notch and impacting with a hammer. Finally, the obtained SEN specimens were loaded in a 3PB configuration using a screw-driven Instron machine (model 8848) at a crosshead speed of 2.0 mm/min and a span of 50 mm. The load–displacement curves were recorded and the maximum loads upon fracture were used to determine the K_{IC} values that were an average of the results for tests run on at least six specimens. Fracture surfaces were subsequently observed using scanning electron microscopy (SEM).

The double-edge-notch four-point bending (DEN-4PB) tool is an effective tool for obtaining information concerning the fracture behavior of polymers.[23] The objective of this technique is to produce two cracks in which one has failed and another has been subcritically loaded. The latter retains an accumulated damage at a point just before failure. The obtained plates were machined into specimens with a dimension of $6 \times 12 \times 110$ mm^3. Two nearly identical cracks were generated on the same edge of the rectangular specimen with a distance of 30 mm. The specimen was then loaded on to the 4PB geometry with a span of 90 mm until one of the cracks failed. Although the two cracks experienced identical stresses, the two cracks cannot be exactly identical. One crack will propagate unstably, leaving the other crack with a nearly critically developed process zone at its tip, which can provide useful information of the process zone upon failure.

Characterization

X-ray diffraction (XRD) patterns were obtained using a GADDS X-ray diffractometer with Cu–K_α radiation ($\lambda = 0.15418$ nm). The XRD was operated at 40 kV and 40 mA. Thin sections ($\sim$ 70 nm thick) were cut using a Leica (Wetzlar, Germany) ultramicrotome equipped with a diamond knife. The clay morphology was studied using a transmission electron microscope (TEM, CM300-FEG, Philips, Eindhoven, The Netherlands) under an accelerated voltage of 150 kV. The fracture surfaces of the SEN-3PB specimens were coated with a thin layer of gold to improve conductivity. The fracture morphology was investigated using an SEM (JSM6700F, JEOL, Tokyo, Japan) at an accelerating voltage of 5 kV and a working distance of 8 mm. Dynamic mechanical analysis (DMA) experiments were performed using a TA Instruments (New Castle, DE) DMA 2980 under a tension mode at a frequency of 1 Hz and a heating rate of 3°C/min. Each sample for DMA measurement was machined to a geometry of $2 \times 10 \times 30$ mm^3.

To scrutinize the morphology of the process zone preceding failure around the subcritically loaded crack tip damage zone, optical microscopy was adopted for morphological investigations on the dam-

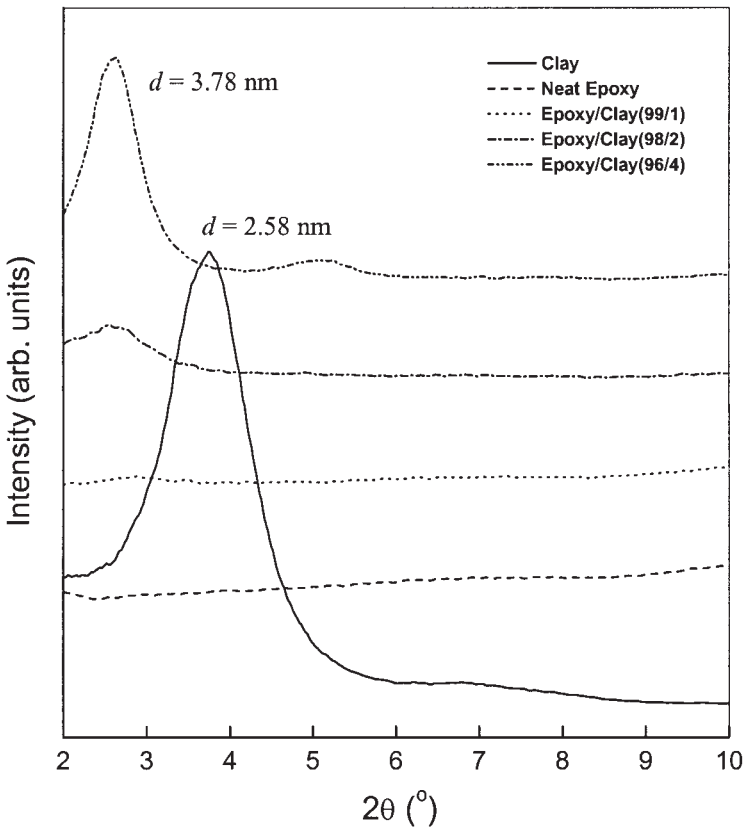

Figure 1 XRD patterns of organoclay, neat epoxy, and the nanocomposites containing different clay concentrations.

aged regions of fractured DEN-4PB specimens. These specimens were polished using rough to fine silicon carbide (SiC) grinding discs (with different grit sizes of 120, 320, 600, 1200, 2400, 4000) and alumina suspensions (3, 1, 0.25 μm), until surface scratches were eliminated. The obtained petrographic thin sections (thickness $<$ 100 μm) were examined using transmitted optical microscopy (TOM).[24]

RESULTS AND DISCUSSION

Clay morphology within epoxy

Figure 1 presents the XRD patterns of the organoclay, neat epoxy, and the nanocomposites containing 1, 2, and 4 wt % of clay. For organoclay, the reflection peak at $2\theta = 3.8°$ (d-spacing = 2.58 nm) is assigned to the (001) basal plane, which corresponds to an interlayer spacing of the clay. The absence of basal reflection in the sample with 1 wt % clay suggests the formation of an exfoliated clay structure after in situ polymerization. However, a small peak at $2\theta = 2.6°$ (d-spacing = 3.78 nm) was observed for the samples with 2 and 4 wt % clay, probably indicating that the clay platelets are not fully exfoliated but intercalated throughout the matrix. However, an XRD pattern with an intercalated peak may not fully reveal extensive levels of exfoliation or intercalation. For example, some clay particles do not display well-defined basal reflections and it is difficult to determine the intensity pattern and the shape of the relative peaks. These considerations make XRD data only a useful approximation to the nanostructure. Hence, XRD is often accompanied by TEM observations, which provide direct visualization of the morphology and spatial distribution of clay platelets.

The clay morphology within epoxy is shown in Figure 2 for the nanocomposite sample containing 2 wt % clay. At lower magnification, clay aggregation is observable as presented in Figure 2(A). The amount of aggregation is dependent on the clay content. At higher loading levels, more clay clusters would be expected. By probing an aggregate at higher magnification [Fig. 2(B)], it can be seen that the clay platelets retain much of their face-to-face alignment but cluster together in large domains. Although there are regions where the regular stacking arrangement is maintained, some other regions, where completely delaminated clay sheets are dispersed individually, can also be seen. Given that a disorientation and delamination of the clay platelets represent exfoliation, the observed morphology may be considered as a mixture of intercalated and exfoliated clay sheets. Although the majority retains their face-to-face orientation, TEM indicates that a small amount of clay does indeed exfoliate. The clay dispersion morphology can also be

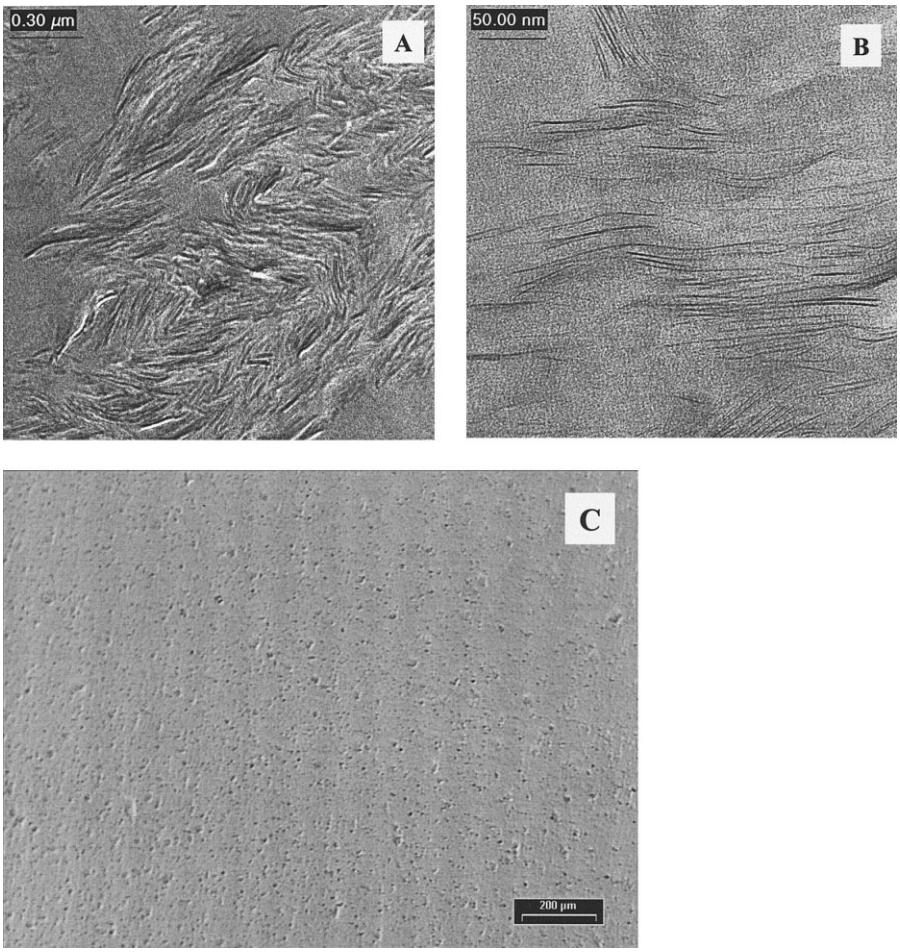

Figure 2 TEM micrographs of an epoxy nanocomposite containing 2 wt % organoclay at low (A) and high (B) magnifications. (C) Optical microscopy showing a homogeneous dispersion of clay aggregates throughout epoxy matrix.

characterized using reflected optical microscopy (ROM) [Fig. 2(C)]. For the epoxy/clay (98/2) system, the clay particles or tactoids (i.e., packets of intercalated clay layers) are homogeneously dispersed in the material with size of about 2–5 μm. A similar morphology of clay agglomerations is often observed by optical microscope and SEM in other epoxy/clay systems.[25–27]

Dynamic mechanical properties

Figure 3(A) illustrates the DMA plots of storage modulus (E) versus temperature as a function of clay concentration. The values of E at 50°C (from the rubbery plateau region) are shown in Figure 3(B). It can be seen that the storage modulus steadily increases as the clay content increases because of an enhancement effect from the addition of rigid inorganic clay particles. Only a moderate increase in storage modulus (by 10%, from 2.49 to 2.75 GPa) was observed as a result of incorporation of 4 wt % clay into the epoxy matrix. However, in a rubbery epoxy matrix, using jeffamine as a curing agent, the improvement in modulus was reported to be much higher ($\sim$ 250%).[28] This clearly indicates that organically modified clay is more effective in reinforcing a soft (rubbery) matrix compared to that in a hard (glassy) matrix. Similar observations have been reported in the literature among various epoxy matrices.[28–32] In addition, compared with the glass-transition temperature (T_g) of neat epoxy resin, that of the nanocomposite decreases by about 10°C (from 168 to 158°C) with increasing clay concentration up to only 4 wt %. This decrease in T_g implies that the molecular motion becomes less restrictive, probably because of a lower degree of crosslinking. The effect of clay addition on the curing behavior of epoxy is still under investigation. Another possible reason for the decrease of T_g of the nanocomposites with increasing clay loading is the plasticization effect from the small molecular organic modifier (surfactant) within the interlayers of the organically modified clay used in this study because the organic loading is up to about 30 wt % from the TGA data (not shown here).[33]

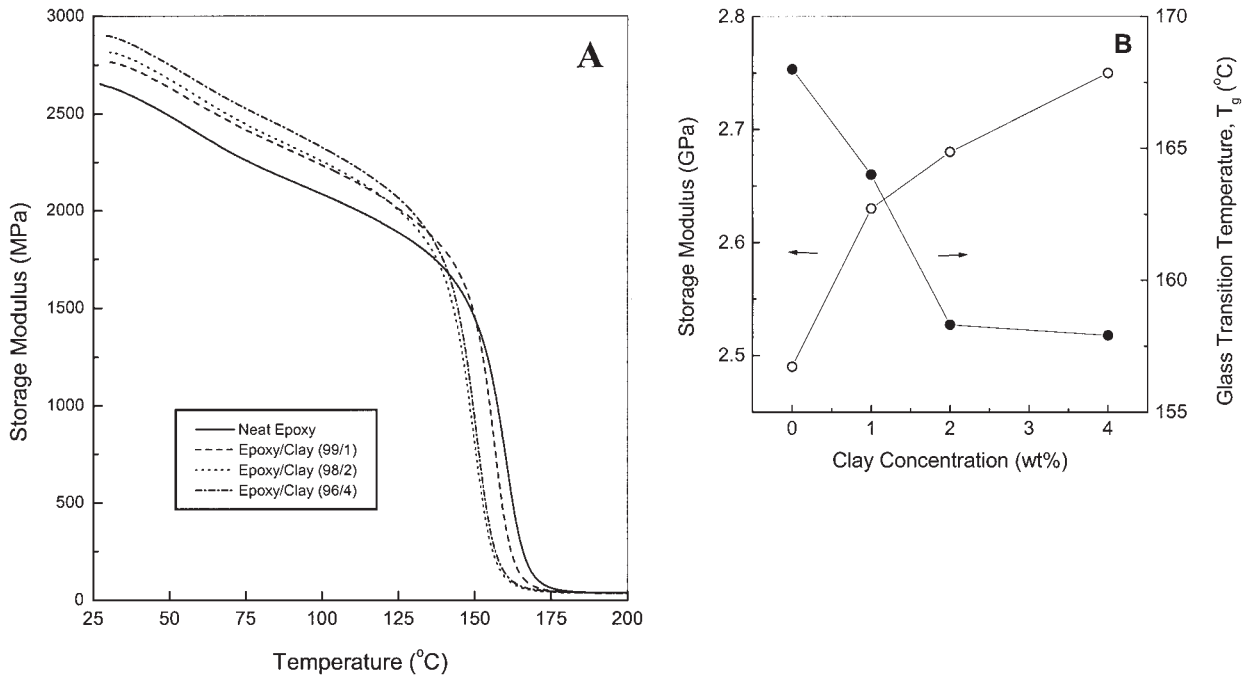

Figure 3 (A) DMA curves and (B) variation of storage modulus (at 50°C) and glass-transition temperature (T_g) of epoxy/clay nanocomposites as a function of clay content.

Fracture behavior and toughening mechanisms

Figure 4(A) shows the typical linear load–displacement curves of 3PB tests for neat epoxy and its nanocomposites. The curves are shifted horizontally for clarity. It can be seen that all the samples fail in a characteristic brittle feature, as evidenced by an abrupt rupture without any yield. The maximum loads are used to calculate the fracture toughness of the specimens. It is known that there are several different ways to estimate toughness, such as (1) the

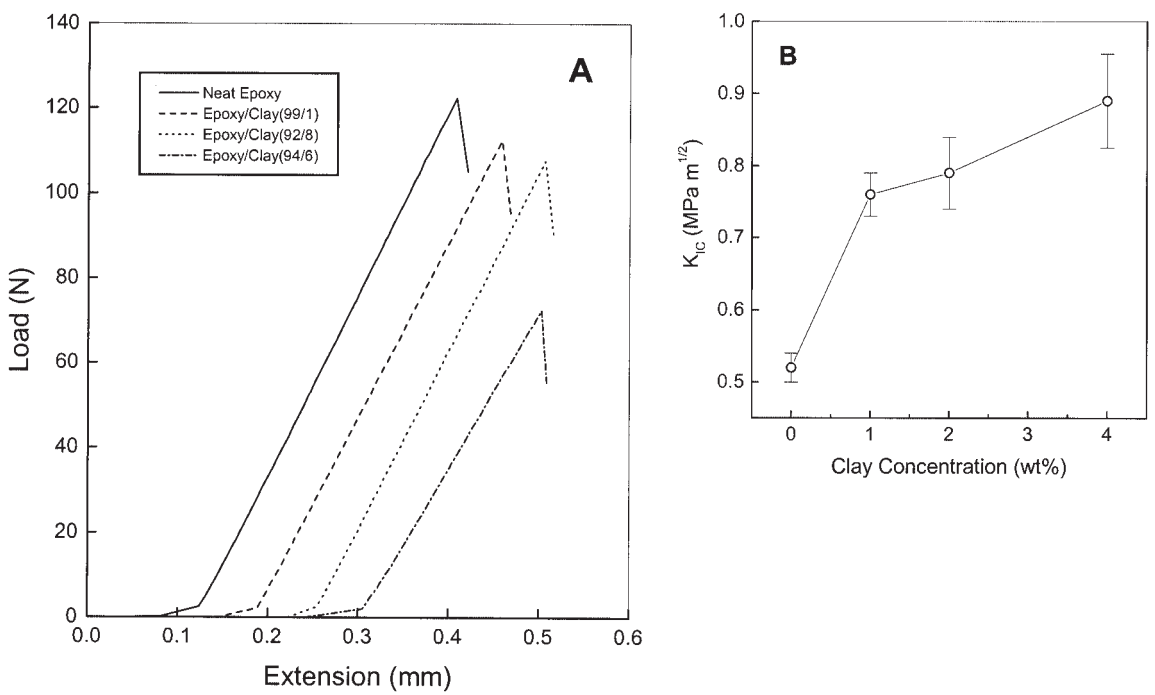

Figure 4 Fracture toughness of epoxy/clay nanocomposites as a function of clay concentration.

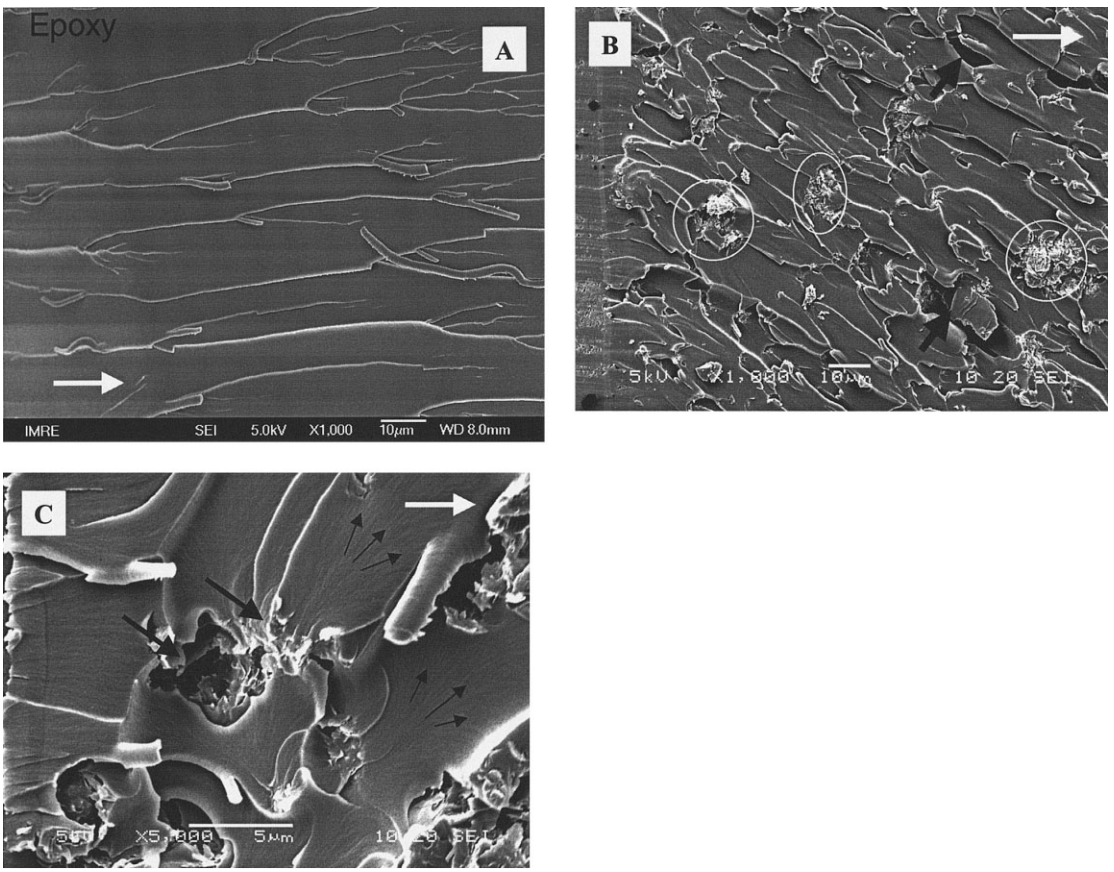

Figure 5 Fracture morphologies within the crack initiation region observed by SEM: (A) neat epoxy; (B) epoxy/clay (98/2), ×1000; (C) epoxy/clay (98/2), ×5000. White arrows indicate the crack propagation direction.

tensile strength, (2) the area under the tensile stress–strain curve, (3) the plain strain/critical strain energy release rate (G_{IC}), or (4) the plain strain/critical stress intensity factor (K_{IC}). The fracture toughness of materials that fail in a brittle manner is usually expressed by K_{IC}, a development of linear elastic fracture mechanics. Therefore, here K_{IC} is used to evaluate the fracture toughness of the intrinsically brittle epoxy and its clay nanocomposites, which is defined by[34,35]

$$K_{IC} = Y\frac{3PS\sqrt{a}}{2BW^2}$$

where Y is a shape factor, P is the load at failure, S is the length of the span, B is the specimen thickness, W is the specimen width, and a is the crack length.

For specific specimen geometry, the shape factor can be determined by the equation

$$Y = 1.93 - 3.07\left(\frac{a}{W}\right) + 14.53\left(\frac{a}{W}\right)^2 - 25.11\left(\frac{a}{W}\right)^3 + 25.8\left(\frac{a}{W}\right)^4$$

Here, Y is a dimensionless parameter that depends on the crack length and specimen sizes. The fracture toughness obtained using the above equations is presented in Figure 4(B). The increase in K_{IC} (by about 70% with only 4 wt % clay) reveals that there is a significant improvement in toughness, indicating that filling epoxy resin with clay particles has a toughening effect and the nanocomposites are appreciably less brittle than the unfilled epoxy resin.

The fracture surfaces of neat epoxy and the nanocomposites were comparatively examined using SEM. Here, only the morphology of crack initiation zone (where stable crack growth occurs) is shown. It can be seen that neat epoxy resin exhibits a relatively smooth fracture surface with cracks in different planes but almost parallel to the crack-propagation direction indicated by a white arrow [Fig. 5(A)]. This indicates a typical fractography feature of brittle fracture behavior, thus accounting for the low fracture toughness of the unfilled epoxy. Compared to the case of neat epoxy, the fracture surfaces of the nanocomposites show considerably different fractographic features. As a representative example, the failure surface of the nanocomposite containing 2 wt % clay is shown in Figure 5(B). Generally, a much rougher fracture surface is seen upon adding clay into the epoxy matrix. The increased surface roughness implies that the path of the crack tip is distorted because of the clay plate-

lets, making crack propagation more difficult. Even though the clay layers are of the order of 1 nm thickness, it has been shown above that many of these systems remain in tactoids. Figure 5(B) also shows that many clay aggregates are observed on the fracture surface, and several distinct agglomerations are indicated by circles. The fact that the lateral clay layers remain micron in dimension means that the clay is readily able to interact with the growing crack front.[36] Therefore, the presence of clay particles or aggregates may cause perturbations along the crack front, thus altering the path of the propagating crack from the straight unperturbed growth seen in the neat resin [Fig. 5(A)], as evidenced by an inclined angle of about 40° relative to the initial crack propagation direction (indicated by a white arrow). Consequently, the cracks are deflected by the clay particles into the rougher regions surrounding them. Clearly, the crack deflection observed is responsible for the increase of fracture toughness by incorporating clay into the epoxy matrix. In addition, the overall textured fracture surface shows a typical tear morphology, indicating that massive plastic deformation of the matrix occurs. Moreover, some microvoids can also be seen on the fracture surfaces, as indicated by black arrows [Fig. 5(B)].

At higher magnification [Fig. 5(C)], a representative fractographic feature, microvoids, can be clearly observed, as indicated by thick black arrows. Upon fracture the clay particles are very likely to be the stress concentration sites, thus usually resulting in (1) debonding of clay–matrix and (2) cleavage of clay tactoids, consequently producing some micro- or nanovoids. These voids could (1) initiate shear yielding of the epoxy matrix at the crack propagation tips and also throughout the entire volume, as indicated by thin black arrows; and (2) deform, absorbing more energy before fracturing. The shear yielding of the matrix is one of several kinds of step structures (such as "lance," "river," and "hackles") contributing to the increase in roughness similarly observed in other epoxy composites, such as glass beads–filled systems.[17,18] Therefore, here both the occurrence of shear yielding and the formation of microvoids are attributed to the increase of fracture toughness for the epoxy/clay nanocomposites. Moreover, it should be noted that the debonding may also occur within clay particles (i.e., clay layer delamination), as observed in some places where the particles are simply cleaved.

Besides SEM observations on the fracture surfaces, TOM was also used to investigate the arrested crack tip damage zone of the DEN-4PB specimens. As demonstrated in Figure 6(A), the unfilled epoxy shows a large (~ hundreds μm) crack tip damage zone, with a sharp and straight path running through the material (with almost no deflection). Therefore, the featureless crack path (almost parallel to the direction of crack propagation) indicates the absence of significant plastic shear deformation. In contrast to neat epoxy, Figure 6(B) manifests small-size (~ tens μm) crack trajectories that are deflected and meandering through the matrix for the nanocomposite containing 2 wt % clay. The TOM observations on the nanocomposite containing 4 wt % clay clearly show a more deflected crack path (not shown here), compared to that of the system with 2 wt % clay. As the clay concentration increases, the distance between the intercalated clay particles decreases, which probably accounts for the crack taking a more tortuous path, either around or between the clay particles. For the crack deflection to occur, the particles need to generate sufficient stress disturbance in front of the crack tip. Thus, when the crack propagates, the crack path will then be altered by the stress disturbance. This implies that an increase in stress disturbance will result in a higher degree of crack deflection. According to the crack-front–bowing mechanism,[18,19] inorganic particles inside the polymer matrix can resist propagation. Thus, when a crack front meets a clay particle, the clay particle acts as an obstruction and causes the crack front to bow. In this case, more energy is required to propagate the crack. Therefore, increasing these "crack stoppers" (i.e., clay loading), the toughness of the material is expected to be improved.

CONCLUSIONS

Epoxy/clay nanocomposites were prepared by dispersing nanoclay particles into the epoxy matrix. XRD and TEM were used to confirm the coexistence of intercalated and exfoliated clay morphology in the nanocomposites. DMA showed that the storage modulus steadily increased, whereas the glass-transition temperature (T_g) of the nanocomposite decreased with increasing clay loading. The presence of small molecule organic surfactant within organoclay interlayers (acting as plasticizers) as well as the unreacted resin (leading to low crosslinking density) probably constitute the reasons for the decrease of T_g.

An increase in the fracture toughness K_{IC} was found with increasing organoclay concentration, indicating that the filling of epoxy resin with organoclay particles has a toughening effect. SEM study showed a rather smooth and flat surface observed for an unfilled epoxy resin, and a dramatic increase in the roughness of the fracture surfaces with increasing clay content, confirming that a great deal of plastic deformation occurred upon failure for epoxy/clay nanocomposites. One possible reason for the toughening mechanism in the intercalated nanocomposite may be attributed to the stress disturbance caused by the clay particles. These clay particles acted as obstacles, causing the crack to take a more tortuous path, either around or between them. The increase in these "crack stoppers" caused the crack to take a more tortuous path, mani-

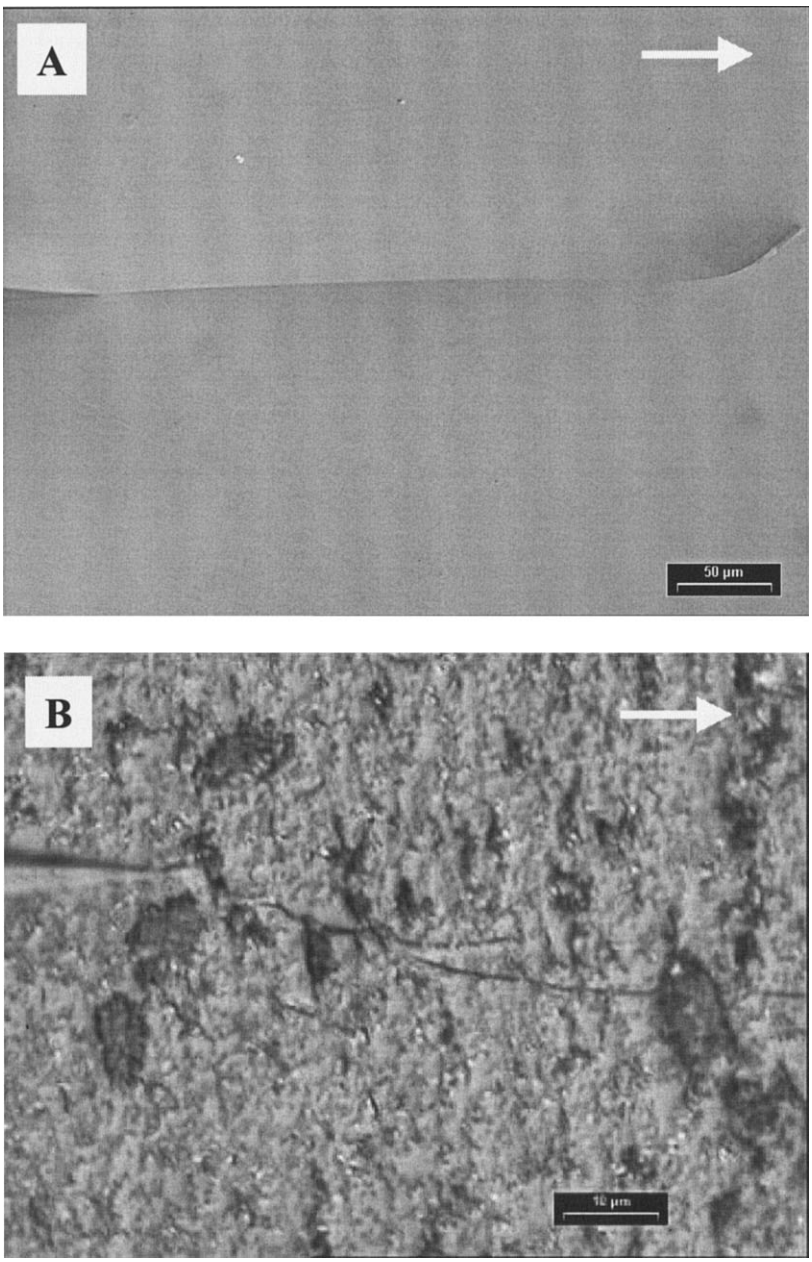

Figure 6 Morphology of the crack tip damage zone by TOM: (A) neat epoxy, ×200; (B) epoxy/clay (96/4) system, ×1000. White arrows indicate the crack propagation direction.

festing a meandering crack trajectory. That is, these inorganic particles inside the polymer matrix have certain resistance to crack propagation. However, when failure occurs in the epoxy/clay systems, more than one toughening mechanism usually occurs, such as shear yielding of the matrix, crack deflection, microvoiding, and debonding observed here by SEM and TOM. Thus, a deeper understanding of the specific factors that influence the crack propagation and fracture behavior would be needed to enable a greater degree of property improvements of the nanocomposites in the future.

References

1. Giannelis, E. P.; Krishnamoorti, R.; Manias, E. Adv Polym Sci 1999, 138, 107.
2. Alexandre, M.; Dubois, P. Mater Sci Eng Rep 2000, 28, 1.
3. Pinnavaia, T. J.; Beal, G. W., Eds. Polymer–Clay Nanocomposites; Wiley: Chichester, 2000.
4. Okada, A.; Kawasumi, M.; Usuki, A.; Kojima, Y.; Kuraucki, T.; Kamigaito, O. Mater Res Soc Proc 1990, 171, 45.
5. Kojima, Y.; Usuki, A.; Kawasumi, M.; Okada, A.; Fukushima, Y.; Kurauchi, T.; Kamigaito, O. J Mater Res 1993, 8, 1185.
6. Shi, H. Z.; Lan, T.; Pinnavaia, T. J. Chem Mater 1996, 8, 1584.
7. Zilg, C.; Dietsche, F.; Hoffmann, B.; Dietrich, C.; Muelhaupt, R. Macromol Symp 2001, 169, 65.

8. Chin, I.-J.; Thurn-Albrecht, T.; Kim, H.-C.; Tussell, T. P.; Wang, J. Polymer 2001, 42, 5947.
9. Salahuddin, N.; Moet, A.; Hiltner, A.; Baer, E. J Appl Polym Sci 2002, 38, 1477.
10. Salahuddin, N.; Moet, A.; Hiltner, A.; Baer, E. Eur Polym J 2002, 38, 1477.
11. Becker, O.; Cheng, Y.-B.; Varley, R. J.; Simon G. P. Macromolecules 2003, 36, 1616.
12. Fu, X.; Qutubuddin, S. Polymer 2001, 42, 807.
13. Vaia, R. A.; Jandt, K. D.; Kramer, E. J.; Giannelis, E. P. Chem Mater 1996, 8, 2628.
14. Bhatnagar, M. S. Polym-Plast Technol 1993, 32, 53.
15. Bhuniya, S.; Adhikari, B. J Appl Polym Sci 2003, 90, 1497.
16. Ratna, D.; Varley, R.; Simon, G. P. J Appl Polym Sci 2003, 89, 2339.
17. Lee, J.; Yee, A. F. Polymer 2000, 41, 8375.
18. Lee, J.; Yee, A. F. Polymer 2001, 42, 577.
19. Manias, E.; Han, W. J.; Jandt, K. D.; Ktamer, E. J.; Giannelis, E. P. Mat Res Soc Symp Proc 1997, 457, 495.
20. Gam, K. T.; Miyamoto, M.; Nishimura, R.; Sue, H.-J. Polym Eng Sci 2003, Oct.
21. Chen, L.; Wong, S. C.; Pisharath, S. J Appl Polym Sci 2003, 88, 3298.
22. Sue, H. J.; Yee, A. F. J Mater Sci 1989, 24, 1447.
23. Pearson, R. A.; Yee, A. F. J Mater Sci 1986, 21, 2475.
24. Lu, J.; Wei, G.-X.; Sue, H.-J.; Chu, J. J Appl Polym Sci 2000, 76, 311.
25. Becker, O.; Varley, R.; Simon, G. Polymer 2002, 43, 4365.
26. Zerda, A.; Lesser, A. J. J Polym Sci Part B: Polym Phys 2001, 39, 1137.
27. Kornmann, X.; Lindberg, H.; Berglund, L. A. Polymer 2001, 42, 1303.
28. Wang, M. S.; Pinnavaia, T. J. Chem Mater 1994, 6, 468.
29. Wang, Z.; Pinnavaia, T. J. Chem Mater 1998, 10, 1820.
30. Lan, T.; Pinnavaia, T. J. Chem Mater 1994, 6, 2216.
31. Lan, T.; Kaviratna, P. D.; Pinnavaia, T. J. Polym Mater Sci Eng 1994, 71, 527.
32. Ratna, D.; Manoj, N. R.; Varley, R.; Singh Raman, R. K.; Simon, G. P. Polym Int 2003, 52, 1403.
33. Liu, T. X.; Lim, K. P.; Tjiu, W. C.; Pramoda, K. P.; Chen, Z.-K. Polymer 2003, 44, 3529.
34. Hertzberg, R. W. Deformation and Fracture Mechanics of Engineering Materials; Wiley: New York, 1989.
35. Lee, J.; Yee, A. F. J Appl Polym Sci 2001, 79, 1371.
36. Becker, O.; Varley, R. J.; Simon, G. P. J Mater Sci Lett 2003, 22, 1411.